Universal and Efimov trimers in an alkaline-earth-metal and alkali-metal gas mixture with spin-orbit coupling

Qing Ji,[1] Ren Zhang,[2,*] and Wei Zhang[1,3,†]
[1]Department of Physics, Renmin University of China, Beijing 100872, China
[2]School of Physics, Xi'an Jiaotong University, Shaanxi 710049, China
[3]Beijing Key Laboratory of Opto-electronic Functional Materials and Micro-nano Devices, Renmin University of China, Beijing 100872, China

(Received 22 October 2020; accepted 23 November 2020; published 9 December 2020)

We exactly solve the two-body and three-body problems in the mixture of alkaline-earth-metal(like) (AE) and alkali-metal atomic gases in the presence of three-dimensional isotropic spin-orbit (SO) coupling. The SO coupling is implemented by the Raman scheme that couples the ground state of the AE atom with different nuclear spin. The interaction between AE and alkali-metal atoms is tuned to be near resonant by Feshbach resonance, while the interaction between the two AE atoms is negligible. We present the Skorniakov–Ter-Martirosian (STM) equation for the three-body system composed of two SO coupled AE atoms and one alkali-metal atom. By solving the STM equation in the zero angular momentum sector, we obtain the energy spectrum and find a nonuniversal Efimov trimer and a universal Kartavtsev-Malykh (KM) trimer in different parameter windows of the mass ratio. In the region where the KM trimer is present, strong SO coupling can stabilize the KM trimer to be the ground state, such that experimental realization and observation can be expected.

DOI: 10.1103/PhysRevA.102.063313

I. INTRODUCTION

The mixture of ultracold atomic gas provides a new perspective for the study of few- and many-body physics, where the atomic mass ratio and statistics can be controlled with high flexibility. Many dual-element alkali-metal and alkaline-earth-metal(like) (AE) atomic gas mixtures have been cooled to quantum degeneracy, including the Bose-Bose mixture [1–3], the Fermi-Fermi mixture [4], and the Bose-Fermi mixture [5–11]. In particular, the recent realization of a mixture of alkali-metal and AE atoms has attracted increasing interest [12,13]. Such a system is a promising platform to simulate the $p_x + ip_y$ topological superfluid and Kondo physics [14,15]. The Feshbach resonances between alkali-metal and AE atoms were successfully observed by an experimental group from Amsterdam [16], unlocking even more opportunities for the investigation of novel few- and many-body quantum phenomena. Near these Feshbach resonances, the interaction is almost independent of the nuclear spin of the AE atoms, such that the system acquires an approximate SU(N) symmetry of nuclear spins.

The synthetic spin-orbit (SO) coupling realized between two hyperfine states of alkali-metal atoms by Raman coupling has greatly enriched the tool kit of ultracold atomic gases [17–23] and has advanced the study of topological quantum states and novel superfluid phases [24–27]. From the viewpoint of the few-body physics, such a technique also supplies a new knob to control two- and three-body bound states. Specifically, in the presence of SO coupling, the two-body bound state becomes more favorable due to the enhancement of the low-energy density of states [28]. For the case of three-body problems, previous works found two types of three-body bound states, i.e., the Efimov trimer and the universal Kartavtsev-Malykh (KM) trimer, and the latter state is energetically more favorable than the former option [29–31]. In addition, the conventional scaling law for the usual Efimov trimer vanishes owing to the presence of SO coupling, while a generalized radical scaling law still exists [30,32].

The Raman scheme of SO coupling is also extended to the system of AE atoms, where two of the nuclear spin states labeled by (↑, ↓) are coupled [33,34]. In this paper, we focus on the three-body system composited by one alkali-metal atom and two fermionic AE atoms with nuclear spins up and down, which are coupled by a three-dimensional isotropic SO coupling. Thanks to the Feshbach resonance between AE and alkali-metal atoms, the interspecies interaction can be tuned to be much larger than that between the two AE atoms, such that the latter can be safely neglected. Moreover, due to the SU(N) symmetry, the interaction between AE and alkali-metal atoms is taken to be identical for the two nuclear spin states of AE atoms. By solving the two-body and three-body problems of such a system, we find that the SO coupling enhances the existence of the two-body bound state, and more importantly, the nonuniversal Efimov trimer and universal KM trimer with a generalized scaling law can be obtained in different parameter windows of the mass ratio.

This paper is arranged as follows. In Sec. II, we present a brief review of the SO coupled two-body problems and emphasize the enhancement of low-energy density of states by SO coupling. In Sec. III, we present the derivation of the

*renzhang@xjtu.edu.cn
†wzhangl@ruc.edu.cn

general Skorniakov–Ter-Martirosian (STM) equation, which is further simplified in Sec. IV by noticing the conservation of total angular momentum. We then derive the partial-wave STM equation and obtain a solvable integral equation for the three-body eigenenergy in the zero total angular momentum sector. In Sec. V, we numerically solve for the eigenenergy of trimer states and analyze the mass-ratio effect on the existence and stability of Efimov and KM trimers. Finally, a summary is presented in Sec. VI.

II. TWO-BODY BOUND STATES

Before embarking on the three-body problem, let us briefly review the solutions to the two-body problems of an SO coupled AE atom and an alkali-metal atom. The two-body Hamiltonian is written as

$$\begin{aligned}\hat{H}_{2b} &= \hat{H}^0_{2b} + \hat{V}_{12},\\ \hat{H}^0_{2b} &= \frac{\hat{\mathbf{p}}_1}{2m} + \frac{\hat{\mathbf{p}}_2^2}{2M} - \frac{\lambda\hat{\mathbf{p}}_2\cdot\hat{\boldsymbol{\sigma}}}{M},\\ \hat{V}_{12} &= g\delta(\mathbf{r}_1-\mathbf{r}_2)\mathbb{I},\end{aligned} \tag{1}$$

where $\hat{\mathbf{p}}_1$ and $\mathbf{r}_1$ are, respectively, the momentum and coordinate operators of the alkali-metal atom with mass m and $\hat{\mathbf{p}}_2$ and $\mathbf{r}_2$ are the corresponding operators of the AE atom with mass M. The momentum of the AE atom is SO coupled to its spin operator $\hat{\boldsymbol{\sigma}}$ spanned by the $\uparrow$ and $\downarrow$ nuclear spin states via an isotropic form with strength λ. The interaction between the alkali-metal and AE atoms $\hat{V_{12}}$ is assumed to be independent of the nuclear spin states and proportional to the identity matrix $\mathbb{I}$ in spin space. In the following discussion, we define the mass ratio as $\mu \equiv M/m$. The interaction strength g is related to the s-wave scattering length a_s via the renormalization relation

$$\frac{1}{g} = \frac{Mm}{2\pi(M+m)a_s} - \frac{1}{\Omega}\sum_{\mathbf{k}}\frac{2Mm}{k^2(M+m)}, \tag{2}$$

where the natural unit $\hbar = 1$ is taken for simplicity, Ω is the quantization volume, and a_s can be controlled by Feshbach resonance [16].

Since the interaction is invariant under the spin rotation, it is diagonal in the basis $\{|\mathbf{k},\uparrow\rangle, |\mathbf{k},\downarrow\rangle\}$, with $\mathbf{k}$ being the relative momentum. Nevertheless, the SO coupling breaks the spin-rotation symmetry. It is straightforward to prove that the kinetic Hamiltonian is diagonal in the helicity basis $\{|\mathbf{k}_1;\mathbf{k}_2,\alpha\rangle\}$, with $\alpha = \pm$ and

$$|\mathbf{k}_1;\mathbf{k}_2,\alpha\rangle = \sum_{\sigma=\uparrow,\downarrow}\gamma^{\sigma}_{\mathbf{k}_2,\alpha}|\mathbf{k}_1;\mathbf{k}_2,\sigma\rangle, \tag{3}$$

where the coefficients are defined as $\gamma^{\uparrow}_{\mathbf{k},+} = e^{-i\frac{\phi_\mathbf{k}}{2}}\cos\frac{\theta_\mathbf{k}}{2}$, $\gamma^{\downarrow}_{\mathbf{k},+} = e^{i\frac{\phi_\mathbf{k}}{2}}\sin\frac{\theta_\mathbf{k}}{2}$, $\gamma^{\uparrow}_{\mathbf{k},-} = -e^{-i\frac{\phi_\mathbf{k}}{2}}\sin\frac{\theta_\mathbf{k}}{2}$, and $\gamma^{\downarrow}_{\mathbf{k},-} = e^{i\frac{\phi_\mathbf{k}}{2}}\cos\frac{\theta_\mathbf{k}}{2}$. Here, $\theta_\mathbf{k}$ and $\phi_\mathbf{k}$ are the azimuthal angles of $\mathbf{k}$. The total momentum of the two-body system is a conserved quantity, and the eigenstate with total momentum $\mathbf{K}$ can, in general, be written as

$$|\Psi_{2b}\rangle = \sum_{\alpha=\pm}\int d\mathbf{k}\psi_\alpha(\mathbf{K}-\mathbf{k}_2;\mathbf{k}_2)|\mathbf{K}-\mathbf{k}_2;\mathbf{k}_2,\alpha\rangle. \tag{4}$$

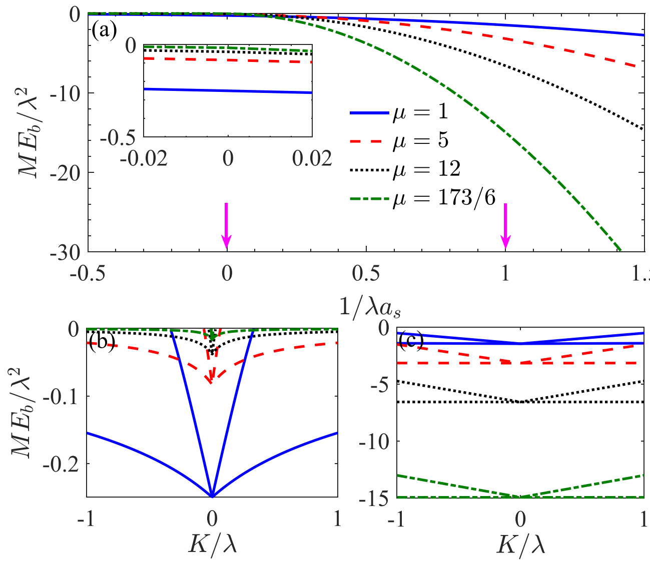

FIG. 1. Two-body binding energy E_b as a function of (a) s-wave scattering length a_s and (b) and (c) SOC strength λ for different mass ratios μ. For (a), the total momentum $|\mathbf{K}| = 0$. For (b) and (c) we take $1/(\lambda a_s) = 0$, 1, respectively, as denoted by the pink arrows. There are two bound states at small $|\mathbf{K}|$, and their binding energies are denoted by the same type of curves.

By solving the Lippmann-Schwinger equation, we obtain the algebraic equation for the two-body bound-state energy E (Appendix A)

$$D(E)^2 - Y(E)^2 = 0, \tag{5}$$

where $D(E)$ and $Y(E)$ represent

$$\begin{aligned}D(E) &\equiv -\frac{\mu/a_s - \frac{(\mu|\mathbf{K}|+\lambda)\mathcal{D}_-(E)+(\mu|\mathbf{K}|-\lambda)\mathcal{D}_+(E)}{2|\mathbf{K}|(1+\mu)}}{2\pi(1+\mu)},\\ Y(E) &\equiv -\frac{\mathcal{Y}_+(E)\mathcal{D}_-(E)+\mathcal{Y}_-(E)\mathcal{D}_+(E)}{12\pi(1+\mu)^2\mu K^2}.\end{aligned} \tag{6}$$

The quantities in the expressions above are $\mathcal{D}_\pm(E) = \sqrt{\mu(|\mathbf{K}|\pm\lambda)^2 - 2(1+\mu)(ME+\lambda)^2}$ and $\mathcal{Y}_\pm(E) = \mu(K^2 \pm \lambda|\mathbf{K}| + \lambda^2) + 3\mu^2K^2 - 2(1+\mu)(ME+\lambda^2)$. Without loss of generality, we choose $\lambda > 0$ hereafter.

By solving Eq. (5), we obtain the two-body bound-state spectrum. In Fig. 1, we show the binding energy $E_b = E - E^{(2b)}_{\rm th}$ as the function of interaction strength and total momentum for different mass ratios, where $E^{(2b)}_{\rm th} = (|\mathbf{K}| - \lambda)^2/2(M+m) - \lambda^2/2M$. In Fig. 1(a), we illustrate the binding energy as a function of s-wave scattering length a_s for the $|\mathbf{K}| = 0$ sector. Notice that a bound state exists even in the BCS regime with $a_s < 0$. This is because the SO coupling enhances the low-energy density of the state [23], which favors the existence of a bound state. However, the mass-ratio dependences of the shallow and deep bound states are quite different.

For the shallow bound state in the BCS regime or near the unitary, the binding energy is smaller than or comparable to λ^2/M. So the SO coupling dominates the interaction when it comes to the bound state. According to Eq. (1), the SO coupling is suppressed when the mass ratio increases. Thus, the binding energy becomes smaller when the mass ratio increases, as shown in the inset of Fig. 1(a). In Fig. 1(b) we show the binding energy with finite total momentum at the unitary. There are two bound states for small $|\mathbf{K}|$, and they are degenerate at $|\mathbf{K}| = 0$. With increasing $|\mathbf{K}|$, one of the bound state disassociates into two atoms. For both of the shallow bound states, the binding energies hold the same dependence on the mass ratio and are both reduced with increasing mass ratio.

For the deeply bound state in the deep Bose-Einstein-condensate regime, the binding energy is much larger than λ^2/M. Then, the SO coupling in this regime is negligible, and the binding energy approximates to

$$E_b \simeq -\frac{1}{Ma_s^2}(1+\mu), \quad \text{as } a_s \to 0^+. \tag{7}$$

Thus, the bound state is enhanced when the mass ratio is increased, as illustrated in Fig. 1(a). Like for the shallow bound state, we calculate the binding energy with finite momentum at $1/(\lambda a_s) = 1$ as shown in Fig. 1(c). There are two bound states as well, and they are degenerate at $|\mathbf{K}| = 0$. In comparison to the BCS regime, here the two bound states are stable in a much wider region of momentum and disassociate into two atoms only at a larger value of $|\mathbf{K}|$.

It is obvious that the binding energy takes its maximum at $|\mathbf{K}| = 0$. The two-body bound-state energies serve as one of the threshold energies for the three-body bound state discussed in the following section.

III. THREE-BODY PROBLEM AND STM EQUATION

For the three-body system composited by two SO coupled AE atoms and one alkali-metal atom, the Hamiltonian is written as $\hat{H}_{3b} = \hat{H}^0_{3b} + \hat{V}_{12} + \hat{V}_{13}$, with

$$\begin{aligned} \hat{H}^0_{3b} &= \frac{\hat{\mathbf{p}}_1^2}{2m} + \sum_{i=2,3}\left(\frac{\hat{\mathbf{p}}_i^2}{2M} - \frac{\lambda\hat{\mathbf{p}}_i\cdot\hat{\sigma}}{M}\right), \\ \hat{V}_{12} &= g\delta(\mathbf{r}_1-\mathbf{r}_2)\mathbb{I}_2\otimes\mathbb{I}_3, \\ \hat{V}_{13} &= g\delta(\mathbf{r}_1-\mathbf{r}_3)\mathbb{I}_2\otimes\mathbb{I}_3. \end{aligned} \tag{8}$$

Here we label the two AE atoms by 2 and 3. $\mathbb{I}_2$ and $\mathbb{I}_3$ are the identities spanned by the spins of the AE-2 and AE-3 atoms, respectively. The other notations are the same as those for the two-body case in the preceding section. Before proceeding further, we would like to emphasize the main difference between our model and the previous ones [29–31]. In Refs. [29,30], the three-body system is composited by two identical fermions and another SO coupled atom, and the interaction exists between fermions and the SO coupled atom. The authors of Ref. [31] considered a system composited by two SO coupled two-component fermions and a third atom. However, the interaction exists only between one of the two components and the third atom. Thus, our system is quite different from these existing works, and we will show that the physics changes as well.

Similar to the two-body problem, the Lippmann-Schwinger equation for the three-body problem is written as

$$|\Psi_{3b}\rangle = \hat{G}_{3b}(\hat{V}_{12}+\hat{V}_{13})|\Psi_{3b}\rangle, \tag{9}$$

where $\hat{G}_{3b} = (E - \hat{H}^0_{3b})^{-1}$ is the free Green's function operator. Notice that Eq. (9) is basis independent; that is, it can be projected to either the helicity basis or the spin basis. Since the free Green's function $\hat{G}_{3b}$ is diagonal in the helicity basis, we project Eq. (9) into the helicity basis and rewrite the wave function as

$$\begin{aligned} &\Psi_{3b}(\mathbf{K}-\mathbf{k}-\mathbf{q};\mathbf{k},\alpha;\mathbf{q},\beta) \\ &\quad = \sum_{\sigma=\uparrow,\downarrow}\frac{F^\sigma_\beta(\mathbf{q})\gamma^{\sigma*}_{\mathbf{k},\alpha} - F^\sigma_\alpha(\mathbf{k})\gamma^{\sigma*}_{\mathbf{q},\beta}}{E - E_0(\mathbf{K}-\mathbf{k}-\mathbf{q};\mathbf{k},\alpha;\mathbf{q},\beta)}. \end{aligned} \tag{10}$$

Here $\alpha,\beta = \pm$ are helicity indices, $\mathbf{K}$ is the total momentum, and

$$\begin{aligned} &E_0(\mathbf{k}_1;\mathbf{k}_2,\alpha;\mathbf{k}_3,\beta) \\ &\quad = \frac{k_1^2}{2m} + \frac{(\mathbf{k}_2+\alpha\lambda)^2}{2M} + \frac{(\mathbf{k}_3+\beta\lambda)^2}{2M} - \frac{\lambda^2}{M} \end{aligned} \tag{11}$$

is the kinetic energy in the presence of SO coupling. The auxiliary function $F^\sigma_\alpha(\mathbf{k})$ is defined as

$$F^\sigma_\alpha(\mathbf{k}) = \frac{g}{(2\pi)^3}\int d\mathbf{q}\sum_{\alpha'}\Psi(\mathbf{K}-\mathbf{k}-\mathbf{q};\mathbf{k},\alpha;\mathbf{q},\alpha')\gamma^\sigma_{\mathbf{q},\alpha'}. \tag{12}$$

By multiplying $\int d\mathbf{k}\sum_{\alpha=\pm}\gamma^\sigma_{\mathbf{k},\alpha}$ on both sides of Eq. (10), we obtain the self-consistent equation for the auxiliary function

$$\begin{aligned} F^\sigma_\beta(\mathbf{q}) &= \sum_{\alpha=\pm}\sum_{\sigma'=\uparrow,\downarrow}\frac{g}{(2\pi)^3} \\ &\quad\times\int d\mathbf{k}\gamma^\sigma_{\mathbf{k},\alpha}\frac{F^{\sigma'}_\beta(\mathbf{q})\gamma^{\sigma'*}_{\mathbf{k},\alpha} - F^{\sigma'}_\alpha(\mathbf{k})\gamma^{\sigma'*}_{\mathbf{q},\beta}}{E - E_0(\mathbf{K}-\mathbf{k}-\mathbf{q};\mathbf{k},\alpha;\mathbf{q},\beta)}. \end{aligned} \tag{13}$$

This is the STM equation for our system. In principle, by solving Eq. (13), one finds the three-body bound-state energy and the corresponding wave function. It is worth pointing out that the STM equation in our system is four-dimensional, which is different from those discussed in Refs. [29,30], where it takes a spinor form.

IV. PARTIAL-WAVE EXPANSION

In the presence of SO coupling, our system still acquires the spatial translational symmetry and a combined symmetry of spatial and spin rotation. Furthermore, we restrict the discussion in the subspace with zero total momentum $\mathbf{K} = 0$, in which case we will have $[\hat{\mathbf{P}}, \hat{\mathbf{J}}] = 0$, and thus, the total angular momenta j and m_j are also conserved quantities, where j and m_j are the eigenvalues corresponding with the total angular momentum operators $\hat{\mathbf{J}}$ and $\hat{J}_z$. However, we stress that our approach can be extended to the general case.

Using the unitary transformation defined in Eq. (3), one can expand the three-body wave function in the spin basis

$$\begin{aligned} &\Psi_{3b}(-\mathbf{k}-\mathbf{q};\mathbf{k},\alpha;\mathbf{q},\beta) \\ &\quad = \sum_{\sigma=\uparrow,\downarrow,\sigma'=\uparrow,\downarrow}\gamma^{\sigma*}_{\mathbf{k},\alpha}\gamma^{\sigma'*}_{\mathbf{q},\beta}\psi_{3b}(-\mathbf{k}-\mathbf{q};\mathbf{k},\sigma;\mathbf{q},\sigma'), \end{aligned} \tag{14}$$

where $\psi_{3b}(-\mathbf{k}-\mathbf{q};\mathbf{k},\sigma;\mathbf{q},\sigma')$ is the three-body wave function component, which can be further expanded as follows:

$$\begin{aligned}\psi_{3b}(-\mathbf{k}-\mathbf{q};\mathbf{k},\sigma;\mathbf{q},\sigma') &= \sum_{(j_i,J_i)}\sum_{(m_{j_i},m_{J_i})}\varphi_{j_1,j_2,J_1,J_2}(k,q)\\ &\times\left[\left\langle j_1,m_{j_1};\frac{1}{2},\sigma\middle|J_1,m_{J_1}\right\rangle\left\langle j_2,m_{j_2};\frac{1}{2},\sigma'\middle|J_2,m_{J_2}\right\rangle\right.\\ &\left.\times\langle J_1,m_{J_1};J_2,m_{J_2}|j,m_j\rangle Y_{j_1}^{m_{j_1}}(\Omega_\mathbf{k})Y_{j_2}^{m_{j_2}}(\Omega_\mathbf{q})\right]. \qquad (15)\end{aligned}$$

In the above expression, $j_i, J_i = 0, 1, 2, \ldots$ respectively label the quantum numbers of the orbital and total angular momenta of particle $i = 1, 2$, while $m_{j_i} = -j_i, -j_i+1, \ldots, j_i-1, j_i$ and $m_{J_i} = -J_i, -J_i+1, \ldots, J_i-1, J_i$ are the corresponding magnetic quantum numbers. In addition, $\Omega_\mathbf{k}$ denotes the solid angle of $\mathbf{k}$, and $Y_{j_i}^{m_{j_i}}(\Omega_\mathbf{k})$ denotes the spherical harmonic function. Substituting Eqs. (14) and (15) into Eq. (12), we obtain the partial-wave component of the auxiliary function and hence the three-body wave function. The expansion in Eq. (15) is valid as long as the total angular momentum is conserved. Thus, our derivation, in principle, is applicable to any j sector.

In the following discussion, we assume that the total angular momentum is zero, that is, $j = m_j = 0$, and $F_\alpha^\sigma(\mathbf{k})$ can be significantly simplified. In such a case, we have $J_1 = J_2$ and $m_{J_1} = -m_{J_2}$. Moreover, since only the s-wave interaction is considered in our system, integration over $\mathbf{q}$ in Eq. (12) leads to $j_2 = m_{j_2} = 0$. Then, we find $J_1 = J_2 = 1/2$ and $m_{J_1} = -m_{J_2} = -\sigma'$, which leads to (i) $j_1 = 0, m_{j_1} = 0$ and (ii) $j_2 = 1, m_{j_2} = \pm 1, 0$. A straightforward calculation shows that

$$F_+^\uparrow(\mathbf{k}) = -\gamma_{\mathbf{k},-}^\uparrow\left(\frac{f_0(k)Y_0^0(\Omega_\mathbf{k})}{\sqrt{2}}+\frac{f_1(k)Y_1^0(\Omega_\mathbf{k})}{\sqrt{6}}\right)-\frac{\gamma_{\mathbf{k},-}^\downarrow f_1(k)Y_1^{-1}(\Omega_\mathbf{k})}{\sqrt{3}}, \qquad (16)$$

$$F_+^\downarrow(\mathbf{k}) = -\gamma_{\mathbf{k},-}^\downarrow\left(\frac{f_0(k)Y_0^0(\Omega_\mathbf{k})}{\sqrt{2}}-\frac{f_1(k)Y_1^0(\Omega_\mathbf{k})}{\sqrt{6}}\right)+\frac{\gamma_{\mathbf{k},-}^\uparrow f_1(k)Y_1^{1}(\Omega_\mathbf{k})}{\sqrt{3}}, \qquad (17)$$

$$F_-^\uparrow(\mathbf{k}) = \gamma_{\mathbf{k},+}^\uparrow\left(\frac{f_0(k)Y_0^0(\Omega_\mathbf{k})}{\sqrt{2}}+\frac{f_1(k)Y_1^0(\Omega_\mathbf{k})}{\sqrt{6}}\right)+\frac{\gamma_{\mathbf{k},-}^\downarrow f_1(k)Y_1^{-1}(\Omega_\mathbf{k})}{\sqrt{3}}, \qquad (18)$$

$$F_-^\downarrow(\mathbf{k}) = \gamma_{\mathbf{k},+}^\downarrow\left(\frac{f_0(k)Y_0^0(\Omega_\mathbf{k})}{\sqrt{2}}-\frac{f_1(k)Y_1^0(\Omega_\mathbf{k})}{\sqrt{6}}\right)-\frac{\gamma_{\mathbf{k},+}^\uparrow f_1(k)Y_1^{1}(\Omega_\mathbf{k})}{\sqrt{3}}, \qquad (19)$$

where $f_0(k)$ and $f_1(k)$ are the functions to be determined by the STM equation (13). It should be noticed that there are only two instead of four linearly independent functions, and this simplification exists only in the $j = 0$ sector.

To obtain the equation for $f_0(k)$ and $f_1(k)$, we substitute Eqs. (16)–(19) into Eq. (13) and obtain the partial-wave STM equation (Appendix B)

$$\begin{aligned}&\begin{bmatrix}W_+(k)-D_+(k) & 0\\ 0 & W_-(k)+D_-(k)\end{bmatrix}\begin{bmatrix}f_+(k)\\ f_-(k)\end{bmatrix}\\ &= \int_0^\Lambda\frac{q^2dq}{(2\pi)^3}\begin{bmatrix}K_0^{-,-}(k,q)-K_1^{-,-}(k,q) & -K_0^{+,-}(k,q)-K_1^{+,-}(k,q)\\ K_0^{-,+}(k,q)+K_1^{-,+}(k,q) & K_1^{+,+}(k,q)-K_0^{+,+}(k,q)\end{bmatrix}\begin{bmatrix}f_+(q)\\ f_-(q)\end{bmatrix}, \qquad (20)\end{aligned}$$

where Λ is the three-body parameter [35–37], $f_\pm(k) \equiv f_1(k) \pm f_0(k)$, and

$$\begin{aligned}D_\pm(k) = -\frac{1}{2\pi(1+\mu)}&\left\{\frac{\mu}{a_s}-\frac{(\mu k+\lambda)\sqrt{\mu(k-\lambda)^2+(1+\mu)[k^2-2(ME+\lambda^2)\mp 2k\lambda+\lambda^2]}}{2(1+\mu)k}\right.\\ &\left.-\frac{(\mu k-\lambda)\sqrt{\mu(k+\lambda)^2+(1+\mu)[k^2-2(ME+\lambda^2)\mp 2k\lambda+\lambda^2)]}}{2(1+\mu)k}\right\}, \qquad (21)\end{aligned}$$

$$\begin{aligned}W_\pm(k) = -\frac{1}{12\pi(1+\mu)^2k^2}&(\{(2k^2+k\lambda+\lambda^2)+4\mu k^2-(1+\mu)[2(mE+\lambda^2/\mu)-(1/\mu-1)k^2\pm 2k\lambda/\mu-\lambda^2/\mu)]\}\\ &\times\sqrt{\mu(k-\lambda)^2+(1+\mu)\mu(k^2-2(mE+\lambda^2/\mu)+(1/\mu-1)k^2\mp 2k\lambda/\mu+\lambda^2/\mu)}\\ &-\{(2k^2-k\lambda+\lambda^2)+4\mu k^2-(1+\mu)[2(mE+\lambda^2/\mu)-(1/\mu-1)k^2\pm 2k\lambda/\mu-\lambda^2/\mu]\}\\ &\times\sqrt{\mu(k+\lambda)^2+(1+\mu)\mu[k^2-2(mE+\lambda^2/\mu)+(1/\mu-1)k^2\mp 2k\lambda/\mu+\lambda^2/\mu]}), \qquad (22)\end{aligned}$$

$$\begin{aligned}K_0^{\alpha=\pm,\beta=\pm} &= \frac{\pi}{kq}\ln\left[1+\frac{4\mu kq}{2ME-(k+\alpha\lambda)^2-(q+\beta\lambda)^2-\mu(k+q)^2}\right],\\ K_1^{\alpha=\pm,\beta=\pm} &= -\frac{2\pi}{kq}+\pi\frac{2ME-(k+\alpha\lambda)^2-(q+\beta\lambda)^2-\mu(k^2+q^2)}{2\mu k^2q^2}\\ &\quad\times\ln\left[1+\frac{4\mu kq}{2ME-(k+\alpha\lambda)^2-(q+\beta\lambda)^2-\mu(k+q)^2}\right]. \qquad (23)\end{aligned}$$

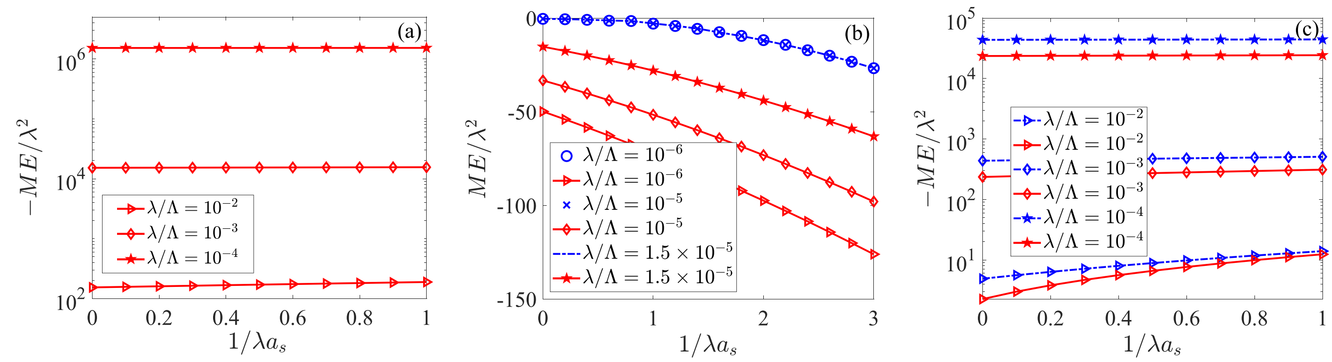

FIG. 2. Three-body bound-state energy as a function of the s-wave scattering length for different mass ratios. (a) $\mu = 5$. There exist only nonuniversal three-body bound states. (b) $\mu = 12$. One universal bound state (blue dashed line, circles, and crosses) and a nonuniversal bound state coexist, and the universal one is the shallowest. (c) $\mu = 173/6$. There are two sets of nonuniversal bound states.

The physical meaning of Eq. (20) can be understood as follows. For the case $\lambda = 0$, Eq. (20) can be significantly simplified as

$$\left[\frac{1}{a_s} - \frac{\sqrt{(1+2\mu)k^2 - 2\mu(1+\mu)E}}{1+\mu}\right] f_l(k) = \frac{2(-1)^{l+1}}{\pi} \int_0^\Lambda q^2 dq K_l^0(k,q) f_l(q), \tag{24}$$

where the index $l = 0, 1$ and

$$K_l^0(k,q) = \int_0^{2\pi} d\theta_{\mathbf{kq}} \frac{P_l(\cos\theta_{\mathbf{kq}})\sin\theta_{\mathbf{kq}}}{2\mu E - k^2 - q^2 - \mu(\mathbf{k}+\mathbf{q})^2}, \tag{25}$$

with $\theta_{\mathbf{kq}}$ denoting the angle between $\mathbf{k}$ and $\mathbf{q}$. Clearly, $f_0(k)$ represents the wave function of a three-body system composed of interacting identical bosons with angular momentum $l = 0$, and $f_1(k)$ is the wave function of a three-body system of two-component fermions with angular momentum $l = 1$. It is known that in the three-boson system nonuniversal Efimov states with a discrete scaling law exist [38]. In the three-body system of two-component fermions, however, the universal KM trimers with a continuous scaling law exist. The first KM trimer emerges when the mass ratio $\mu \geqslant 8.172$, and the second one appears when $12.917 \leqslant \mu < 13.606$. If the mass ratio is further increased beyond 13.606, Efimov trimers start to emerge [35–37,39–41].

Our system is composited of three distinguishable particles with s-wave interaction. In the absence of SO coupling, the sectors with angular momentum $l = 0$ and $l = 1$ thus correspond to the bosonic and fermionic systems, respectively. When the SO coupling is turned on, the total angular momentum j becomes a good quantum number. In the $j = 0$ sector, $f_0(k)$ and $f_1(k)$ are coupled by SO coupling, as indicated by Eq. (20).

V. MASS-RATIO EFFECT AND EFIMOVIAN SCALING LAW

By solving Eq. (20), we obtain the three-body bound-state energy and show the result as a function of the s-wave scattering length a_s for different mass ratios μ in Fig. 2, from which one can easily observe different types of three-body bound states for different mass ratios. When the mass ratio is small, a series of nonuniversal three-body bound states whose binding energies are dependent on the three-body parameter Λ exists, as can be found in Fig. 2(a) for $\mu = 5$. With increasing the mass ratio to $\mu = 12$, a KM trimer emerges, as illustrated by the blue dashed curve in Fig. 2(b). The bound-state energy of that KM trimer is apparently independent of the three-body parameter. By further increasing the mass ratio, the universal KM trimer disappears, and more nonuniversal trimers emerge, as depicted in Fig. 2(c), where a mixture of ^{173}Yb and ^{6}Li is considered as an example. The nonuniversal trimers fall into two classes labeled by the red (light gray) and blue (dark gray) curves. Our results so far are qualitatively consistent with the case without SO coupling, i.e., $\lambda = 0$, where the nonuniversal trimers are the Efimov states with discrete scaling law. Two natural questions then arise in the presence of SO coupling: (1) Is the nonuniversal trimer still the Efimov state? (2) If so, does the scaling law need to be modified?

To address these two questions, we calculate the three-body bound-state energy as a function of the SO coupling strength λ for different mass ratios. In the absence of SO coupling, the KM trimer satisfies the continuous scaling law $a_s \to \xi a_s$, $E \to \xi^{-2}E$. Thus, the three-body bound-state energy $E = 0$ at unitarity. However, for the Efimov trimer, the three-body parameter breaks the continuous scaling law into a discrete scaling law. In Fig. 3, we confirm these statements at $\lambda = 0$. As indicated by the red (medium gray) squares in Fig. 3(a) and red (medium gray) and blue (dark gray) squares in Fig. 3(c), the scaling law in such circumstances reads $E_{n+1}/E_n = e^{2\pi/s_0^l}$, where the superscript $l = 0, 1$ corresponds to the total orbital angular momentum and $s_0^0 \approx 0.997$ for $\mu = 5$, $s_0^0 \approx 2.243$, and $s_0^1 \approx 1.650$ for $\mu = 173/6$. For the case $\mu = 12$, a universal KM trimer (blue dash-dotted lines) and nonuniversal trimers (red solid lines) with $s_0^0 \approx 1.499$ exist.

When the SO coupling ramps up, we observe that the three-body bound-state energy becomes larger, which is also owing to the enhancement of the low-energy density of states by SO coupling. The three-body bound state eventually merges to the two-body bound state (green dashed curves in Fig. 3) for sufficiently strong SO coupling. As indicated in Ref. [30], the three-body bound states $\psi(e^{-\pi/s_0^l}\mathbf{R})$ and $\psi(\mathbf{R})$ satisfy the

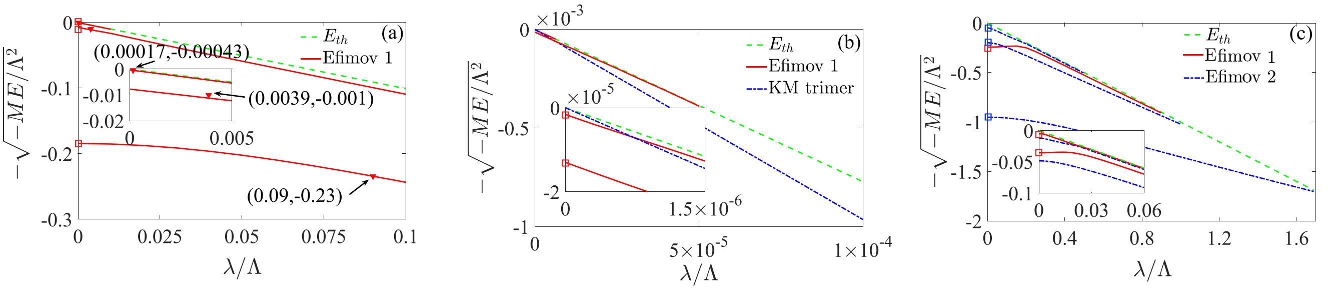

FIG. 3. Three-body bound-state energy as a function of the SO coupling strength λ for different mass ratios. The inset shows results near $\lambda/\Lambda = 0$. (a) $\mu = 5$ and $1/(\lambda a_s) = 0$; the Efimov trimers represented by the red triangles satisfy the scaling law in Eq. (27) with $s_0^0 \approx 0.997$. (b) $\mu = 12$ and $1/(\lambda a_s) = 3$. There exists an Efimov trimer with $s_0^0 \approx 1.499$ and a universal KM trimer, and the latter is energetically favorable at sufficiently strong SO coupling. In our calculation, Λ is large enough that the universal KM trimer energies have converged. (c) $\mu = 173/6$ and $1/(\lambda a_s) = 0$. There exists a series of Efimov trimers which fall into two classes denoted by red solid and blue dash-dotted curves with $s_0^0 \approx 2.243$ and $s_0^1 \approx 1.650$, respectively.

same Shrödinger equation if we perform the following scaling transformation:

$$E \to E e^{2\pi/s_0^l}, \quad \lambda \to \lambda e^{\pi/s_0^l},$$
$$a_s \to a_s e^{-\pi/s_0^l}, \quad \mathbf{R} \to \mathbf{R} e^{-\pi/s_0^l}. \tag{26}$$

As a result, the nonuniversal trimer energy satisfies the scaling law

$$\frac{E_{n+1}(\lambda, a_s)}{E_n\left(\lambda e^{\pi/s_0^l}, a_s e^{-\pi/s_0^l}\right)} = e^{-2\pi/s_0^l}. \tag{27}$$

In Fig. 3(a), we verified this scaling relation as indicated by the three red triangles. So the nonuniversal trimers in our system are the Efimov states with a modified discrete scaling law which involves SO coupling. When the mass ratio is larger than the critical value, the KM trimer appears which satisfies the continuous scaling law,

$$E \to \xi^{-2} E, \quad \lambda \to \xi^{-1}\lambda, \quad a_s \to \xi a_s. \tag{28}$$

Using $\mu = 12$ as an example, we illustrate the KM trimer and Efimov trimer in Fig. 3(b). The energy of the KM trimer does not rely on the three-body parameter Λ, and thus, all the points $(\lambda/\Lambda, -\sqrt{-ME/\Lambda^2})$ should fall onto a straight line pointing to the origin, which is the case in Fig. 3(b), as shown by the blue dash-dotted line. As can be seen in the inset, the Efimov trimer is energetically favorable when the SO coupling is weak. By increasing the SO coupling λ beyond a critical value at which the Efimov and KM trimers are generated, the KM trimer becomes the ground state. When the mass ratio is further increased, the KM trimer vanishes, and more Efimov states appear, as shown in Fig. 3(c) with mass ratio $\mu = 173/6$.

The degeneracy between the KM and Efimov trimers shown in Fig. 3(b) can be understood by noticing that the two states acquire different scaling symmetries. While the Efimov trimer is discretely scaling invariant, the KM trimer is continuously scaling invariant. As the discrete scaling symmetry is a subset of the continuous scaling symmetry, the degenerate energies for different Efimov branches should exhibit the same discrete scaling law as in Eq. (26), which is confirmed by our numerical results.

VI. SUMMARY

In summary, we exactly solved the two- and three-body problems in a mixture of alkaline-earth-metal and alkali-metal atoms. In such a system, the nuclear-spin-independent Feshbach resonance is used to tune the interaction between the AE and alkali-metal atoms. The SO coupling is realized by coupling the nuclear spin of AE atoms via the clock transition or the Raman transition. We find a nonuniversal Efimov trimer and/or universal KM trimer within a different range of mass ratios between AE and alkali-metal atoms. When the mass ratio $\mu = M/m$ between the SO coupled AE atom M and the alkali-metal atom m is small, a series of Efimov states with a discrete scaling law exists. By increasing the mass ratio beyond a critical value, a universal KM trimer emerges and coexists with the Efimov trimers. The KM trimer is energetically more favorable than the Efimov trimer for strong enough SO coupling, such that it can be realized and observed in the experiment. If the mass ratio is further increased, the KM trimer vanishes, and an extra series of Efimov trimers emerges. In Table I, we illustrate the difference between the systems that support the KM trimer. Our study enriches the understanding of SO coupled few-body systems.

TABLE I. Comparison of SO coupling three-body systems in different studies.

Composited particle	SO coupling configuration	Interaction	Ref.
Two identical fermions + one spin-$\frac{1}{2}$ atom	Imposed on one spin-$\frac{1}{2}$ atom	Between fermions and the spin-$\frac{1}{2}$ atom	[29,30]
Two spin-$\frac{1}{2}$ fermions $(\uparrow, \downarrow)$ + one spinless atom	Imposed on two spin-$\frac{1}{2}$ atoms	Between fermions $(\uparrow)$ and the spinless atom	[31]
Two spin-$\frac{1}{2}$ fermions $(\uparrow, \downarrow)$ + one spinless atom	Imposed on two spin-$\frac{1}{2}$ atoms	Between fermions $(\uparrow, \downarrow)$ and the spinless atom	This paper

ACKNOWLEDGMENTS

We are grateful to Z.-Y. Shi and W. Yi for helpful discussions. This work is supported by the National Key R&D Program of China [Grants No. 2018YFA0307601 (R.Z.) and No. 2018YFA0306501 (W.Z.)], the National Natural Science Foundation of China (Grants No. 11434011, No. 11522436, No. 11704408, No. 11774425, and No. 11804268), the Beijing Natural Science Foundation (Grant No. Z180013), the Joint Fund of the Ministry of Education (Grand No. 6141A020333xx), the Research Funds of Renmin University of China (Grants No. 16XNLQ03 and No. 18XNLQ15), the Fundamental Research Funds for the Central Universities, and the Research Funds of Renmin University of China.

APPENDIX A: TWO-BODY BOUND-STATE DERIVATION

In the two-body part we consider an alkali-metal atom (denoted as **1**) interacting with an AE atom (denoted as **2**), and the AE atom is subject to isotropic spin-orbit coupling. The two-body Hamiltonian is given by Eq. (1) in the main text. In the helicity basis $|\mathbf{k}_1;\mathbf{k}_2,\alpha\rangle$, we have

$$\hat{H}^0_{2\mathrm{b}} = \int d\mathbf{k}_1 d\mathbf{k}_2 \sum_{\alpha=\pm} E^0_{2\mathrm{b}}(\mathbf{k}_1;\mathbf{k}_2,\alpha)|\mathbf{k}_1;\mathbf{k}_2,\alpha\rangle\langle\mathbf{k}_1;\mathbf{k}_2,\alpha|,$$

$$\hat{V}_{12} = \frac{g}{(2\pi)^3}\int d\mathbf{K}d\mathbf{k_1}d\mathbf{k_2}\sum_{\alpha=\pm}|\mathbf{K}-\mathbf{k_1};\mathbf{k_1},\alpha\rangle\langle\mathbf{K}-\mathbf{k_2};\mathbf{k_2},\alpha|, \tag{A1}$$

with $E^0_{2\mathrm{b}}(\mathbf{k}_1;\mathbf{k}_2,\alpha) = \frac{k_1^2}{2m} + \frac{(k_2-\alpha\lambda)^2}{2M} - \frac{\lambda^2}{2M}$.

We solve the two-body problem through the Lippman-Schwinger equation

$$|\Psi_{2\mathrm{b}}\rangle = \hat{G}_{2\mathrm{b}}\hat{V}_{12}|\Psi_{2\mathrm{b}}\rangle, \tag{A2}$$

where $|\Psi_{2\mathrm{b}}\rangle$ is the two-body bound state given by Eq. (4) and the two-body Green's function $\hat{G}_{2\mathrm{b}}$ reads

$$\hat{G}_{2\mathrm{b}} = \int d\mathbf{k}_1 d\mathbf{k}_2 \sum_{\alpha=\pm}\frac{1}{E-E^0_{2b}(\mathbf{k}_1;\mathbf{k}_2,\alpha)}|\mathbf{k}_1;\mathbf{k}_2,\alpha\rangle\langle\mathbf{k}_1;\mathbf{k}_2,\alpha|. \tag{A3}$$

Multiplying $\langle\mathbf{K}-\mathbf{k_2};\mathbf{k_2},\alpha|$ on both sides, we get the wave function with total momentum $\mathbf{K}$,

$$\Psi_{2b}(\mathbf{K}-\mathbf{k_2};\mathbf{k_2},\alpha) = \int \frac{g}{(2\pi)^3}\frac{d\mathbf{k}'\sum_{\alpha',\sigma}\Psi_{2b}(\mathbf{K}-\mathbf{k}';\mathbf{k}',\alpha')\gamma^{\sigma*}_{\mathbf{k_2},\alpha}\gamma^{\sigma}_{\mathbf{k}',\alpha'}}{E-E^0_{2b}(\mathbf{K}-\mathbf{k_2};\mathbf{k_2},\alpha)}, \tag{A4}$$

where $\gamma^{\sigma}_{\mathbf{k},\alpha}$ is defined in Sec II. Defining the auxiliary function

$$f^{\sigma}_{\mathbf{K}} = \frac{g}{(2\pi)^3}\int d\mathbf{k_2}\sum_{\alpha}\Psi_{2b}(\mathbf{K}-\mathbf{k_2};\mathbf{k_2},\alpha)\gamma^{\sigma}_{\mathbf{k_2},\alpha}, \tag{A5}$$

we have

$$\Psi_{2b}(\mathbf{K}-\mathbf{k_2};\mathbf{k_2},\alpha)\gamma^{\sigma}_{\mathbf{k_2},\alpha} = \frac{1}{E-E^0_{2b}(\mathbf{K}-\mathbf{k_2};\mathbf{k_2},\alpha)}\sum_{\sigma'}f^{\sigma'}_{\mathbf{K}}\gamma^{\sigma'*}_{\mathbf{k_2},\alpha}\gamma^{\sigma}_{\mathbf{k_2},\alpha}. \tag{A6}$$

Then we can obtain the self-consistent equation satisfied by $f^{\sigma}_{\mathbf{K}}$,

$$f^{\sigma}_{\mathbf{K}} = \frac{g}{(2\pi)^3}\int d\mathbf{k_2}\sum_{\sigma'}G^{\sigma,\sigma'}_{2\mathrm{b}}(\mathbf{K}-\mathbf{k_2};\mathbf{k_2})f^{\sigma'}_{\mathbf{K}}, \tag{A7}$$

i.e.,

$$\frac{1}{(2\pi)^3}\int d\mathbf{k}\begin{pmatrix} G^{\uparrow\uparrow}_{2\mathrm{b}}(\mathbf{K}-\mathbf{k_2};\mathbf{k_2}) - \frac{1}{g} & G^{\uparrow\downarrow}_{2\mathrm{b}}(\mathbf{K}-\mathbf{k_2};\mathbf{k_2}) \\ G^{\downarrow\uparrow}_{2\mathrm{b}}(\mathbf{K}-\mathbf{k_2};\mathbf{k_2}) & G^{\downarrow\downarrow}_{2\mathrm{b}}(\mathbf{K}-\mathbf{k_2};\mathbf{k_2}) - \frac{1}{g}\end{pmatrix}\begin{pmatrix} f^{\uparrow}_{\mathbf{K}} \\ f^{\downarrow}_{\mathbf{K}}\end{pmatrix} = 0, \tag{A8}$$

with $G^{\sigma\sigma'}_{2\mathrm{b}}$ defined as

$$G^{\sigma\sigma'}_{2\mathrm{b}}(\mathbf{K}-\mathbf{k_2};\mathbf{k_2}) = \sum_{\alpha}\frac{\gamma^{\sigma'*}_{\mathbf{k_2},\alpha}\gamma^{\sigma}_{\mathbf{k_2},\alpha}}{E-E^0_{2b}(\mathbf{K}-\mathbf{k_2};\mathbf{k_2},\alpha)}. \tag{A9}$$

By further calculation, we can simplify Eq. (A8) into

$$\begin{pmatrix} D(E)+Y(E)\cos\theta & Y(E)\sin\theta e^{-i\phi} \\ Y(E)\sin\theta e^{i\phi} & D(E)-Y(E)\cos\theta\end{pmatrix}\begin{pmatrix} f^{\uparrow}_{\mathbf{K}} \\ f^{\downarrow}_{\mathbf{K}}\end{pmatrix} = 0, \tag{A10}$$

where θ and ϕ stand for $\theta_{\mathbf{K}}$ and $\phi_{\mathbf{K}}$, $D(E)$ and $Y(E)$ are defined as in the main text, and $\mu \equiv \frac{M}{m}$ is the mass ratio. The two-body bound-state energy E is determined by Eq. (5).

APPENDIX B: PARTIAL-WAVE STM EQUATION

To simplify the STM equation as given by Eq. (13), we derive its partial-wave expansion form in this Appendix.

We first rewrite the auxiliary function $F_\alpha^\sigma(\mathbf{k})$ in a variable separated form in terms of the harmonic functions. Substituting Eqs. (14) and (15) into the auxiliary function (12), we can obtain the partial-wave expression of the auxiliary functions,

$$
\begin{aligned}
F_+^\uparrow(\mathbf{k}) = {}& \gamma_{\mathbf{k},-}^{\downarrow}\big[\langle 0,0;\tfrac{1}{2},\tfrac{1}{2}\big|\tfrac{1}{2},\tfrac{1}{2}\rangle\langle j-1,m_j-1;\tfrac{1}{2},\tfrac{1}{2}\big|j-\tfrac{1}{2},m_j-\tfrac{1}{2}\rangle\langle\tfrac{1}{2},\tfrac{1}{2};j-\tfrac{1}{2},m_j-\tfrac{1}{2}\big|j,m_j\rangle f_3(k)Y_{j-1}^{m_j-1}(\Omega_{\mathbf{k}})\\
&+\langle 0,0;\tfrac{1}{2},\tfrac{1}{2}\big|\tfrac{1}{2},\tfrac{1}{2}\rangle\langle j,m_j-1;\tfrac{1}{2},\tfrac{1}{2}\big|j-\tfrac{1}{2},m_j-\tfrac{1}{2}\rangle\langle\tfrac{1}{2},\tfrac{1}{2};j-\tfrac{1}{2},m_j-\tfrac{1}{2}\big|j,m_j\rangle f_2(k)Y_{j}^{m_j-1}(\Omega_{\mathbf{k}})\\
&+\langle 0,0;\tfrac{1}{2},\tfrac{1}{2}\big|\tfrac{1}{2},\tfrac{1}{2}\rangle\langle j,m_j-1;\tfrac{1}{2},\tfrac{1}{2}\big|j+\tfrac{1}{2},m_j-\tfrac{1}{2}\rangle\langle\tfrac{1}{2},\tfrac{1}{2};j+\tfrac{1}{2},m_j-\tfrac{1}{2}\big|j,m_j\rangle f_0(k)Y_{j}^{m_j-1}(\Omega_{\mathbf{k}})\\
&+\langle 0,0;\tfrac{1}{2},\tfrac{1}{2}\big|\tfrac{1}{2},\tfrac{1}{2}\rangle\langle j+1,m_j-1;\tfrac{1}{2},\tfrac{1}{2}\big|j+\tfrac{1}{2},m_j-\tfrac{1}{2}\rangle\langle\tfrac{1}{2},\tfrac{1}{2};j+\tfrac{1}{2},m_j-\tfrac{1}{2}\big|j,m_j\rangle f_1(k)Y_{j+1}^{m_j-1}(\Omega_{\mathbf{k}})\big]\\
&-\gamma_{\mathbf{k},-}^{\uparrow}\big[\langle 0,0;\tfrac{1}{2},\tfrac{1}{2}\big|\tfrac{1}{2},\tfrac{1}{2}\rangle\langle j-1,m_j;\tfrac{1}{2},-\tfrac{1}{2}\big|j-\tfrac{1}{2},m_j-\tfrac{1}{2}\rangle\langle\tfrac{1}{2},\tfrac{1}{2};j-\tfrac{1}{2},m_j-\tfrac{1}{2}\big|j,m_j\rangle f_3(k)Y_{j-1}^{m_j}(\Omega_{\mathbf{k}})\\
&+\langle 0,0;\tfrac{1}{2},\tfrac{1}{2}\big|\tfrac{1}{2},\tfrac{1}{2}\rangle\langle j,m_j;\tfrac{1}{2},-\tfrac{1}{2}\big|j-\tfrac{1}{2},m_j-\tfrac{1}{2}\rangle\langle\tfrac{1}{2},\tfrac{1}{2};j-\tfrac{1}{2},m_j-\tfrac{1}{2}\big|j,m_j\rangle f_2(k)Y_{j}^{m_j}(\Omega_{\mathbf{k}})\\
&+\langle 0,0;\tfrac{1}{2},\tfrac{1}{2}\big|\tfrac{1}{2},\tfrac{1}{2}\rangle\langle j,m_j;\tfrac{1}{2},-\tfrac{1}{2}\big|j+\tfrac{1}{2},m_j-\tfrac{1}{2}\rangle\langle\tfrac{1}{2},\tfrac{1}{2};j+\tfrac{1}{2},m_j-\tfrac{1}{2}\big|j,m_j\rangle f_0(k)Y_{j}^{m_j}(\Omega_{\mathbf{k}})\\
&+\langle 0,0;\tfrac{1}{2},\tfrac{1}{2}\big|\tfrac{1}{2},\tfrac{1}{2}\rangle\langle j+1,m_j;\tfrac{1}{2},-\tfrac{1}{2}\big|j+\tfrac{1}{2},m_j-\tfrac{1}{2}\rangle\langle\tfrac{1}{2},\tfrac{1}{2};j+\tfrac{1}{2},m_j-\tfrac{1}{2}\big|j,m_j\rangle f_1(k)Y_{j+1}^{m_j}(\Omega_{\mathbf{k}})\big],\\
F_+^\downarrow(\mathbf{k}) = {}& \gamma_{\mathbf{k},-}^{\downarrow}\big[\langle 0,0;\tfrac{1}{2},-\tfrac{1}{2}\big|\tfrac{1}{2},-\tfrac{1}{2}\rangle\langle j-1,m_j;\tfrac{1}{2},\tfrac{1}{2}\big|j-\tfrac{1}{2},m_j+\tfrac{1}{2}\rangle\langle\tfrac{1}{2},-\tfrac{1}{2};j-\tfrac{1}{2},m_j+\tfrac{1}{2}\big|j,m_j\rangle f_3(k)Y_{j-1}^{m_j}(\Omega_{\mathbf{k}})\\
&+\langle 0,0;\tfrac{1}{2},-\tfrac{1}{2}\big|\tfrac{1}{2},-\tfrac{1}{2}\rangle\langle j,m_j;\tfrac{1}{2},\tfrac{1}{2}\big|j-\tfrac{1}{2},m_j+\tfrac{1}{2}\rangle\langle\tfrac{1}{2},-\tfrac{1}{2};j-\tfrac{1}{2},m_j+\tfrac{1}{2}\big|j,m_j\rangle f_2(k)Y_{j}^{m_j}(\Omega_{\mathbf{k}})\\
&+\langle 0,0;\tfrac{1}{2},-\tfrac{1}{2}\big|\tfrac{1}{2},-\tfrac{1}{2}\rangle\langle j,m_j;\tfrac{1}{2},\tfrac{1}{2}\big|j+\tfrac{1}{2},m_j+\tfrac{1}{2}\rangle\langle\tfrac{1}{2},-\tfrac{1}{2};j+\tfrac{1}{2},m_j+\tfrac{1}{2}\big|j,m_j\rangle f_0(k)Y_{j}^{m_j}(\Omega_{\mathbf{k}})\\
&+\langle 0,0;\tfrac{1}{2},-\tfrac{1}{2}\big|\tfrac{1}{2},-\tfrac{1}{2}\rangle\langle j+1,m_j;\tfrac{1}{2},\tfrac{1}{2}\big|j+\tfrac{1}{2},m_j+\tfrac{1}{2}\rangle\langle\tfrac{1}{2},-\tfrac{1}{2};j+\tfrac{1}{2},m_j+\tfrac{1}{2}\big|j,m_j\rangle f_1(k)Y_{j+1}^{m_j}(\Omega_{\mathbf{k}})\big]\\
&-\gamma_{\mathbf{k},-}^{\uparrow}\big[\langle 0,0;\tfrac{1}{2},-\tfrac{1}{2}\big|\tfrac{1}{2},-\tfrac{1}{2}\rangle\langle j-1,m_j+1;\tfrac{1}{2},-\tfrac{1}{2}\big|j-\tfrac{1}{2},m_j+\tfrac{1}{2}\rangle\langle\tfrac{1}{2},-\tfrac{1}{2};j-\tfrac{1}{2},m_j+\tfrac{1}{2}\big|j,m_j\rangle f_3(k)Y_{j-1}^{m_j+1}(\Omega_{\mathbf{k}})\\
&+\langle 0,0;\tfrac{1}{2},-\tfrac{1}{2}\big|\tfrac{1}{2},-\tfrac{1}{2}\rangle\langle j,m_j+1;\tfrac{1}{2},-\tfrac{1}{2}\big|j-\tfrac{1}{2},m_j+\tfrac{1}{2}\rangle\langle\tfrac{1}{2},-\tfrac{1}{2};j-\tfrac{1}{2},m_j+\tfrac{1}{2}\big|j,m_j\rangle f_2(k)Y_{j}^{m_j+1}(\Omega_{\mathbf{k}})\\
&+\langle 0,0;\tfrac{1}{2},-\tfrac{1}{2}\big|\tfrac{1}{2},-\tfrac{1}{2}\rangle\langle j,m_j+1;\tfrac{1}{2},-\tfrac{1}{2}\big|j+\tfrac{1}{2},m_j+\tfrac{1}{2}\rangle\langle\tfrac{1}{2},-\tfrac{1}{2};j+\tfrac{1}{2},m_j+\tfrac{1}{2}\big|j,m_j\rangle f_0(k)Y_{j}^{m_j+1}(\Omega_{\mathbf{k}})\\
&+\langle 0,0;\tfrac{1}{2},-\tfrac{1}{2}\big|\tfrac{1}{2},-\tfrac{1}{2}\rangle\langle j+1,m_j+1;\tfrac{1}{2},-\tfrac{1}{2}\big|j+\tfrac{1}{2},m_j+\tfrac{1}{2}\rangle\langle\tfrac{1}{2},-\tfrac{1}{2};j+\tfrac{1}{2},m_j+\tfrac{1}{2}\big|j,m_j\rangle f_1(k)Y_{j+1}^{m_j+1}(\Omega_{\mathbf{k}})\big],\\
F_-^\uparrow(\mathbf{k}) = {}& \gamma_{\mathbf{k},+}^{\uparrow}\big[\langle 0,0;\tfrac{1}{2},\tfrac{1}{2}\big|\tfrac{1}{2},\tfrac{1}{2}\rangle\langle j-1,m_j;\tfrac{1}{2},-\tfrac{1}{2}\big|j-\tfrac{1}{2},m_j-\tfrac{1}{2}\rangle\langle\tfrac{1}{2},\tfrac{1}{2};j-\tfrac{1}{2},m_j-\tfrac{1}{2}\big|j,m_j\rangle f_3(k)Y_{j-1}^{m_j}(\Omega_{\mathbf{k}})\\
&+\langle 0,0;\tfrac{1}{2},\tfrac{1}{2}\big|\tfrac{1}{2},\tfrac{1}{2}\rangle\langle j,m_j;\tfrac{1}{2},-\tfrac{1}{2}\big|j-\tfrac{1}{2},m_j-\tfrac{1}{2}\rangle\langle\tfrac{1}{2},\tfrac{1}{2};j-\tfrac{1}{2},m_j-\tfrac{1}{2}\big|j,m_j\rangle f_2(k)Y_{j}^{m_j}(\Omega_{\mathbf{k}})\\
&+\langle 0,0;\tfrac{1}{2},\tfrac{1}{2}\big|\tfrac{1}{2},\tfrac{1}{2}\rangle\langle j,m_j;\tfrac{1}{2},-\tfrac{1}{2}\big|j+\tfrac{1}{2},m_j-\tfrac{1}{2}\rangle\langle\tfrac{1}{2},\tfrac{1}{2};j+\tfrac{1}{2},m_j-\tfrac{1}{2}\big|j,m_j\rangle f_0(k)Y_{j}^{m_j}(\Omega_{\mathbf{k}})\\
&+\langle 0,0;\tfrac{1}{2},\tfrac{1}{2}\big|\tfrac{1}{2},\tfrac{1}{2}\rangle\langle j+1,m_j;\tfrac{1}{2},-\tfrac{1}{2}\big|j+\tfrac{1}{2},m_j-\tfrac{1}{2}\rangle\langle\tfrac{1}{2},\tfrac{1}{2};j+\tfrac{1}{2},m_j-\tfrac{1}{2}\big|j,m_j\rangle f_1(k)Y_{j+1}^{m_j}(\Omega_{\mathbf{k}})\big]\\
&-\gamma_{\mathbf{k},+}^{\downarrow}\big[\langle 0,0;\tfrac{1}{2},\tfrac{1}{2}\big|\tfrac{1}{2},\tfrac{1}{2}\rangle\langle j-1,m_j-1;\tfrac{1}{2},\tfrac{1}{2}\big|j-\tfrac{1}{2},m_j-\tfrac{1}{2}\rangle\langle\tfrac{1}{2},\tfrac{1}{2};j-\tfrac{1}{2},m_j-\tfrac{1}{2}\big|j,m_j\rangle f_3(k)Y_{j-1}^{m_j-1}(\Omega_{\mathbf{k}})\\
&+\langle 0,0;\tfrac{1}{2},\tfrac{1}{2}\big|\tfrac{1}{2},\tfrac{1}{2}\rangle\langle j,m_j-1;\tfrac{1}{2},\tfrac{1}{2}\big|j-\tfrac{1}{2},m_j-\tfrac{1}{2}\rangle\langle\tfrac{1}{2},\tfrac{1}{2};j-\tfrac{1}{2},m_j-\tfrac{1}{2}\big|j,m_j\rangle f_2(k)Y_{j}^{m_j-1}(\Omega_{\mathbf{k}})\\
&+\langle 0,0;\tfrac{1}{2},\tfrac{1}{2}\big|\tfrac{1}{2},\tfrac{1}{2}\rangle\langle j,m_j-1;\tfrac{1}{2},\tfrac{1}{2}\big|j+\tfrac{1}{2},m_j-\tfrac{1}{2}\rangle\langle\tfrac{1}{2},\tfrac{1}{2};j+\tfrac{1}{2},m_j-\tfrac{1}{2}\big|j,m_j\rangle f_0(k)Y_{j}^{m_j-1}(\Omega_{\mathbf{k}})\\
&+\langle 0,0;\tfrac{1}{2},\tfrac{1}{2}\big|\tfrac{1}{2},\tfrac{1}{2}\rangle\langle j+1,m_j-1;\tfrac{1}{2},\tfrac{1}{2}\big|j+\tfrac{1}{2},m_j-\tfrac{1}{2}\rangle\langle\tfrac{1}{2},\tfrac{1}{2};j+\tfrac{1}{2},m_j-\tfrac{1}{2}\big|j,m_j\rangle f_1(k)Y_{j+1}^{m_j-1}(\Omega_{\mathbf{k}})\big],
\end{aligned}
\tag{B1}
$$

$$
\begin{aligned}
F_-^\downarrow(\mathbf{k}) = {}& \gamma_{\mathbf{k},+}^{\uparrow}\big[\langle 0,0;\tfrac{1}{2},-\tfrac{1}{2}\big|\tfrac{1}{2},-\tfrac{1}{2}\rangle\langle j-1,m_j+1;\tfrac{1}{2},-\tfrac{1}{2}\big|j-\tfrac{1}{2},m_j+\tfrac{1}{2}\rangle\langle\tfrac{1}{2},-\tfrac{1}{2};j-\tfrac{1}{2},m_j+\tfrac{1}{2}\big|j,m_j\rangle f_3(k)Y_{j-1}^{m_j+1}(\Omega_{\mathbf{k}})\\
&+\langle 0,0;\tfrac{1}{2},-\tfrac{1}{2}\big|\tfrac{1}{2},-\tfrac{1}{2}\rangle\langle j,m_j+1;\tfrac{1}{2},-\tfrac{1}{2}\big|j-\tfrac{1}{2},m_j+\tfrac{1}{2}\rangle\langle\tfrac{1}{2},-\tfrac{1}{2};j-\tfrac{1}{2},m_j+\tfrac{1}{2}\big|j,m_j\rangle f_2(k)Y_{j}^{m_j+1}(\Omega_{\mathbf{k}})\\
&+\langle 0,0;\tfrac{1}{2},-\tfrac{1}{2}\big|\tfrac{1}{2},-\tfrac{1}{2}\rangle\langle j,m_j+1;\tfrac{1}{2},-\tfrac{1}{2}\big|j+\tfrac{1}{2},m_j+\tfrac{1}{2}\rangle\langle\tfrac{1}{2},-\tfrac{1}{2};j+\tfrac{1}{2},m_j+\tfrac{1}{2}\big|j,m_j\rangle f_0(k)Y_{j}^{m_j+1}(\Omega_{\mathbf{k}})\\
&+\langle 0,0;\tfrac{1}{2},-\tfrac{1}{2}\big|\tfrac{1}{2},-\tfrac{1}{2}\rangle\langle j+1,m_j+1;\tfrac{1}{2},-\tfrac{1}{2}\big|j+\tfrac{1}{2},m_j+\tfrac{1}{2}\rangle\langle\tfrac{1}{2},-\tfrac{1}{2};j+\tfrac{1}{2},m_j+\tfrac{1}{2}\big|j,m_j\rangle f_1(k)Y_{j+1}^{m_j+1}(\Omega_{\mathbf{k}})\big]\\
&-\gamma_{\mathbf{k},+}^{\downarrow}\big[\langle 0,0;\tfrac{1}{2},-\tfrac{1}{2}\big|\tfrac{1}{2},-\tfrac{1}{2}\rangle\langle j-1,m_j;\tfrac{1}{2},\tfrac{1}{2}\big|j-\tfrac{1}{2},m_j+\tfrac{1}{2}\rangle\langle\tfrac{1}{2},-\tfrac{1}{2};j-\tfrac{1}{2},m_j+\tfrac{1}{2}\big|j,m_j\rangle f_3(k)Y_{j-1}^{m_j}(\Omega_{\mathbf{k}})
\end{aligned}
$$

$$+\langle 0,0;\tfrac{1}{2},-\tfrac{1}{2}|\tfrac{1}{2},-\tfrac{1}{2}\rangle\langle j,m_j;\tfrac{1}{2},\tfrac{1}{2}|j-\tfrac{1}{2},m_j+\tfrac{1}{2}\rangle\langle \tfrac{1}{2},-\tfrac{1}{2};j-\tfrac{1}{2},m_j+\tfrac{1}{2}|j,m_j\rangle f_2(k)Y_j^{m_j}(\Omega_{\mathbf{k}})$$
$$+\langle 0,0;\tfrac{1}{2},-\tfrac{1}{2}|\tfrac{1}{2},-\tfrac{1}{2}\rangle\langle j,m_j;\tfrac{1}{2},\tfrac{1}{2}|j+\tfrac{1}{2},m_j+\tfrac{1}{2}\rangle\langle \tfrac{1}{2},-\tfrac{1}{2};j+\tfrac{1}{2},m_j+\tfrac{1}{2}|j,m_j\rangle f_0(k)Y_j^{m_j}(\Omega_{\mathbf{k}})$$
$$+\langle 0,0;\tfrac{1}{2},-\tfrac{1}{2}|\tfrac{1}{2},-\tfrac{1}{2}\rangle\langle j+1,m_j;\tfrac{1}{2},\tfrac{1}{2}|j+\tfrac{1}{2},m_j+\tfrac{1}{2}\rangle\langle \tfrac{1}{2},-\tfrac{1}{2};j+\tfrac{1}{2},m_j+\tfrac{1}{2}|j,m_j\rangle f_1(k)Y_{j+1}^{m_j}(\Omega_{\mathbf{k}})\Big], \tag{B2}$$

which, in principle, can be determined by the new functions $f_{0,1,2,3}(k)$. Nevertheless, we further restrict the angular momentum $(j, m_j) = (0, 0)$, and in this case the partial-wave expression of the auxiliary function can be further simplified into Eqs. (16)–(19).

Next, we substitute Eqs. (16)–(19) into the coupled STM equation (13) and obtain the explicit form

$$\begin{aligned}
&C_1^1(\mathbf{q})F_+^{\uparrow}(\mathbf{q})+C_2^1(\mathbf{q})F_+^{\downarrow}(\mathbf{q})\\
&=\frac{1}{(2\pi)^3}\int d\mathbf{k}\frac{2\mu(\gamma_{\mathbf{q},+}^{\uparrow})^*\gamma_{\mathbf{k},+}^{\uparrow}}{2ME-(k+\lambda)^2-(q+\lambda)^2-\mu(\mathbf{k}+\mathbf{q})^2}F_+^{\uparrow}(\mathbf{k})+\frac{2\mu(\gamma_{\mathbf{q},+}^{\uparrow})^*\gamma_{\mathbf{k},-}^{\uparrow}}{2ME-(k-\lambda)^2-(q+\lambda)^2-\mu(\mathbf{k}+\mathbf{q})^2}F_-^{\uparrow}(\mathbf{k})\\
&\quad+\frac{1}{(2\pi)^3}\int d\mathbf{k}\frac{2\mu(\gamma_{\mathbf{q},+}^{\downarrow})^*\gamma_{\mathbf{k},+}^{\uparrow}}{2ME-(k+\lambda)^2-(q+\lambda)^2-\mu(\mathbf{k}+\mathbf{q})^2}F_+^{\downarrow}(\mathbf{k})+\frac{2\mu(\gamma_{\mathbf{q},+}^{\downarrow})^*\gamma_{\mathbf{k},-}^{\uparrow}}{2ME-(k-\lambda)^2-(q+\lambda)^2-\mu(\mathbf{k}+\mathbf{q})^2}F_-^{\downarrow}(\mathbf{k}),\\
&C_1^2(\mathbf{q})F_+^{\downarrow}(\mathbf{q})+C_2^2(\mathbf{q})F_+^{\uparrow}(\mathbf{q})\\
&=\frac{1}{(2\pi)^3}\int d\mathbf{k}\frac{2\mu(\gamma_{\mathbf{q},+}^{\uparrow})^*\gamma_{\mathbf{k},+}^{\downarrow}}{2ME-(k+\lambda)^2-(q+\lambda)^2-\mu(\mathbf{k}+\mathbf{q})^2}F_+^{\uparrow}(\mathbf{k})+\frac{2\mu(\gamma_{\mathbf{q},+}^{\uparrow})^*\gamma_{\mathbf{k},-}^{\downarrow}}{2ME-(k-\lambda)^2-(q+\lambda)^2-\mu(\mathbf{k}+\mathbf{q})^2}F_-^{\uparrow}(\mathbf{k})\\
&\quad+\frac{1}{(2\pi)^3}\int d\mathbf{k}\frac{2\mu(\gamma_{\mathbf{q},+}^{\downarrow})^*\gamma_{\mathbf{k},+}^{\downarrow}}{2ME-(k+\lambda)^2-(q+\lambda)^2-\mu(\mathbf{k}+\mathbf{q})^2}F_+^{\downarrow}(\mathbf{k})+\frac{2\mu(\gamma_{\mathbf{q},+}^{\downarrow})^*\gamma_{\mathbf{k},-}^{\downarrow}}{2ME-(k-\lambda)^2-(q+\lambda)^2-\mu(\mathbf{k}+\mathbf{q})^2}F_-^{\downarrow}(\mathbf{k}),\\
&C_1^3(\mathbf{q})F_-^{\uparrow}(\mathbf{q})+C_2^3(\mathbf{q})F_-^{\downarrow}(\mathbf{q})\\
&=\frac{1}{(2\pi)^3}\int d\mathbf{k}\frac{2\mu(\gamma_{\mathbf{q},-}^{\uparrow})^*\gamma_{\mathbf{k},+}^{\uparrow}}{2ME-(k+\lambda)^2-(q-\lambda)^2-\mu(\mathbf{k}+\mathbf{q})^2}F_+^{\uparrow}(\mathbf{k})+\frac{2\mu(\gamma_{\mathbf{q},-}^{\uparrow})^*\gamma_{\mathbf{k},-}^{\uparrow}}{2ME-(k-\lambda)^2-(q-\lambda)^2-\mu(\mathbf{k}+\mathbf{q})^2}F_-^{\uparrow}(\mathbf{k})\\
&\quad+\frac{1}{(2\pi)^3}\int d\mathbf{k}\frac{2\mu(\gamma_{\mathbf{q},-}^{\downarrow})^*\gamma_{\mathbf{k},+}^{\uparrow}}{2ME-(k+\lambda)^2-(q-\lambda)^2-\mu(\mathbf{k}+\mathbf{q})^2}F_+^{\downarrow}(\mathbf{k})+\frac{2\mu(\gamma_{\mathbf{q},-}^{\downarrow})^*\gamma_{\mathbf{k},-}^{\uparrow}}{2ME-(k-\lambda)^2-(q-\lambda)^2-\mu(\mathbf{k}+\mathbf{q})^2}F_-^{\downarrow}(\mathbf{k}),\\
&C_1^4(\mathbf{q})F_-^{\downarrow}(\mathbf{q})+C_2^4(\mathbf{q})F_-^{\uparrow}(\mathbf{q})\\
&=\frac{1}{(2\pi)^3}\int d\mathbf{k}\frac{2\mu(\gamma_{\mathbf{q},-}^{\uparrow})^*\gamma_{\mathbf{k},+}^{\downarrow}}{2ME-(k+\lambda)^2-(q-\lambda)^2-\mu(\mathbf{k}+\mathbf{q})^2}F_+^{\uparrow}(\mathbf{k})+\frac{2\mu(\gamma_{\mathbf{q},-}^{\uparrow})^*\gamma_{\mathbf{k},-}^{\downarrow}}{2ME-(k-\lambda)^2-(q-\lambda)^2-\mu(\mathbf{k}+\mathbf{q})^2}F_-^{\uparrow}(\mathbf{k})\\
&\quad+\frac{1}{(2\pi)^3}\int d\mathbf{k}\frac{2\mu(\gamma_{\mathbf{q},-}^{\downarrow})^*\gamma_{\mathbf{k},+}^{\downarrow}}{2ME-(k+\lambda)^2-(q-\lambda)^2-\mu(\mathbf{k}+\mathbf{q})^2}F_+^{\downarrow}(\mathbf{k})+\frac{2\mu(\gamma_{\mathbf{q},-}^{\downarrow})^*\gamma_{\mathbf{k},-}^{\downarrow}}{2ME-(k-\lambda)^2-(q-\lambda)^2-\mu(\mathbf{k}+\mathbf{q})^2}F_-^{\downarrow}(\mathbf{k}),
\end{aligned} \tag{B3}$$

where we have

$$C_1^1(\mathbf{q})=\frac{1}{(2\pi)^3}\int d\mathbf{k}\sum_{\alpha}\frac{1}{E-E_0(-\mathbf{k}-\mathbf{q};\mathbf{k},\alpha;\mathbf{q},+)}(\gamma_{\mathbf{k},\alpha}^{\uparrow})^*\gamma_{\mathbf{k},\alpha}^{\uparrow}-\frac{1}{g}=D_-(q)-W_-(q)\cos\theta_{\mathbf{q}}, \tag{B4}$$

$$C_2^1(\mathbf{q})=\frac{1}{(2\pi)^3}\int d\mathbf{k}\sum_{\alpha}\frac{1}{E-E_0(-\mathbf{k}-\mathbf{q};\mathbf{k},\alpha;\mathbf{q},+)}(\gamma_{\mathbf{k},\alpha}^{\downarrow})^*\gamma_{\mathbf{k},\alpha}^{\uparrow}=-W_-(q)\sin\theta_{\mathbf{q}}e^{-i\phi_{\mathbf{q}}}, \tag{B5}$$

$$C_1^2(\mathbf{q})=\frac{1}{(2\pi)^3}\int d\mathbf{k}\sum_{\alpha}\frac{1}{E-E_0(-\mathbf{k}-\mathbf{q};\mathbf{k},\alpha;\mathbf{q},+)}(\gamma_{\mathbf{k},\alpha}^{\downarrow})^*\gamma_{\mathbf{k},\alpha}^{\downarrow}-\frac{1}{g}=D_-(q)+W_-(q)\cos\theta_{\mathbf{q}}, \tag{B6}$$

$$C_2^2(\mathbf{q})=\frac{1}{(2\pi)^3}\int d\mathbf{k}\sum_{\alpha}\frac{1}{E-E_0(-\mathbf{k}-\mathbf{q};\mathbf{k},\alpha;\mathbf{q},+)}(\gamma_{\mathbf{k},\alpha}^{\uparrow})^*\gamma_{\mathbf{k},\alpha}^{\downarrow}=-W_-(q)\sin\theta_{\mathbf{q}}e^{i\phi_{\mathbf{q}}}, \tag{B7}$$

$$C_1^3(\mathbf{q})=\frac{1}{(2\pi)^3}\int d\mathbf{k}\sum_{\alpha}\frac{1}{E-E_0(-\mathbf{k}-\mathbf{q};\mathbf{k},\alpha;\mathbf{q},-)}(\gamma_{\mathbf{k},\alpha}^{\uparrow})^*\gamma_{\mathbf{k},\alpha}^{\uparrow}-\frac{1}{g}=D_+(q)-W_+(q)\cos\theta_{\mathbf{q}}, \tag{B8}$$

$$C_2^3(\mathbf{q})=\frac{1}{(2\pi)^3}\int d\mathbf{k}\sum_{\alpha}\frac{1}{E-E_0(-\mathbf{k}-\mathbf{q};\mathbf{k},\alpha;\mathbf{q},-)}(\gamma_{\mathbf{k},\alpha}^{\downarrow})^*\gamma_{\mathbf{k},\alpha}^{\uparrow}=-W_+(q)\sin\theta_{\mathbf{q}}e^{-i\phi_{\mathbf{q}}}, \tag{B9}$$

$$C_1^4(\mathbf{q})=\frac{1}{(2\pi)^3}\int d\mathbf{k}\sum_{\alpha}\frac{1}{E-E_0(-\mathbf{k}-\mathbf{q};\mathbf{k},\alpha;\mathbf{q},-)}(\gamma_{\mathbf{k},\alpha}^{\downarrow})^*\gamma_{\mathbf{k},\alpha}^{\downarrow}-\frac{1}{g}=D_+(q)+W_+(q)\cos\theta_{\mathbf{q}}, \tag{B10}$$

$$C_2^4(\mathbf{q}) = \frac{1}{(2\pi)^3}\int d\mathbf{k}\sum_\alpha \frac{1}{E - E_0(-\mathbf{k}-\mathbf{q};\mathbf{k},\alpha;\mathbf{q},-)}(\gamma_{\mathbf{k},\alpha}^{\uparrow})^*\gamma_{\mathbf{k},\alpha}^{\downarrow} = -W_+(q)\sin\theta_{\mathbf{q}}e^{i\phi_{\mathbf{q}}}, \tag{B11}$$

with $D_\pm(k)$ and $W_\pm(k)$ given by Eqs. (21) and (22) respectively. In addition, we expand the following terms as

$$\frac{\mu}{2ME - (k+\alpha\lambda)^2 - (q+\beta\lambda)^2 - \mu(\mathbf{k}+\mathbf{q})^2} = \sum_l a_l^{\alpha,\beta}(k,q)P_l(\cos\theta_{\mathbf{kq}}) = \sum_{l,m} K_l^{\alpha,\beta}(k,q)Y_l^m(\Omega_{\mathbf{q}})\left[Y_l^m(\Omega_{\mathbf{k}})\right]^*, \tag{B12}$$

where P_j is the jth Legendre polynomial and $s_{1,2} = \pm$. Using the relation $P_l(\cos\theta_{\mathbf{kq}}) = \frac{4\pi}{2l+1}\sum_{m=-l}^{l} Y_l^m(\Omega_{\mathbf{q}})[Y_l^m(\Omega_{\mathbf{k}})]^*$ and the orthogonality condition,

$$\int_0^\pi P_n(\cos\theta)P_m(\cos\theta)\sin\theta d\theta = \frac{2}{2n+1}\delta_{mn}, \tag{B13}$$

we can determine the coefficients $a_l^{\alpha,\beta}$, $K_l^{\alpha,\beta}$ as

$$a_l^{\alpha,\beta}(k,q) = \frac{2l+1}{2}\int \sin\theta_{\mathbf{kq}}d\theta_{\mathbf{kq}}P_l(\cos\theta_{\mathbf{kq}})\frac{\mu}{2ME - (k+\alpha\lambda)^2 - (q+\beta\lambda)^2 - \mu(\mathbf{k}+\mathbf{q})^2},$$
$$K_l^{\alpha,\beta}(k,q) = \frac{4\pi}{2l+1}a_l^{\alpha,\beta}(k,q). \tag{B14}$$

Substituting Eqs. (B4)–(B12) and Eqs. (16)–(19) into Eqs. (B3) and combining the restriction $(j, m_j) = (0, 0)$, we obtain the partial-wave STM equations

$$[D_-(q) + W_-(q)][f_0(q) - f_1(q)] = \frac{1}{(2\pi)^3}\int k^2dk\{[K_1^{+,+}(k,q) - K_0^{+,+}(k,q) - K_1^{-,+}(k,q) - K_0^{-,+}(k,q)]f_0(k)$$
$$- [K_1^{+,+}(k,q) - K_0^{+,+}(k,q) + K_1^{-,+}(k,q) + K_0^{-,+}(k,q)]f_1(k)\},$$
$$[W_+(q) - D_+(q)][f_0(q) + f_1(q)] = \frac{1}{(2\pi)^3}\int k^2dk\{[K_1^{+,-}(k,q) - K_1^{-,-}(k,q) + K_0^{+,-}(k,q) + K_0^{-,-}(k,q)]f_0(k)$$
$$+ [K_0^{-,-}(k,q) - K_1^{+,-}(k,q) - K_1^{-,-}(k,q) - K_0^{+,-}(k,q)]f_1(k)\}, \tag{B15}$$

where $K_0^{\alpha=\pm,\beta=\pm}$ and $K_1^{\alpha=\pm,\beta=\pm}$ are given by Eq. (23) in the main text. Redefining

$$f_+(q) = f_1(q) + f_0(q),$$
$$f_-(q) = f_1(q) - f_0(q), \tag{B16}$$

we have

$$[D_-(q) + W_-(q)]f_-(q) = \frac{1}{(2\pi)^3}\int k^2dk\{[K_1^{+,+}(k,q) - K_0^{+,+}(k,q)]f_-(k) + [K_1^{-,+}(k,q) + K_0^{-,+}(k,q)]f_+(k)\},$$
$$[W_+(q) - D_+(q)]f_+(q) = \frac{1}{(2\pi)^3}\int k^2dk\{-[K_1^{+,-}(k,q) + K_0^{+,-}(k,q)]f_-(k) + [K_0^{-,-}(k,q) - K_1^{-,-}(k,q)]f_+(k)\}, \tag{B17}$$

which can be written in the matrix form as given by Eq. (20) in the main text.

[1] A. D. Lercher, T. Takekoshi, M. Debatin, B. Schuster, R. Rameshan, F. Ferlaino, R. Grimm, and H. C. Nägerl, Production of a dual-species Bose-Einstein condensate of Rb and Cs atoms, Eur. Phys. J. D **65**, 3 (2011).

[2] D. J. McCarron, H. W. Cho, D. L. Jenkin, M. P. Köppinger, and S. L. Cornish, Dual-species Bose-Einstein condensate of ^{87}Rb and ^{133}Cs, Phys. Rev. A **84**, 011603(R) (2011).

[3] B. Pasquiou, A. Bayerle, S. M. Tzanova, S. Stellmer, J. Szczepkowski, M. Parigger, R. Grimm, and F. Schreck, Quantum degenerate mixtures of strontium and rubidium atoms, Phys. Rev. A **88**, 023601 (2013).

[4] M. Taglieber, A.-C. Voigt, T. Aoki, T. W. Hänsch, and K. Dieckmann, Quantum Degenerate Two-Species Fermi-Fermi Mixture Coexisting with a Bose-Einstein Condensate, Phys. Rev. Lett. **100**, 010401 (2008).

[5] G. Roati, F. Riboli, G. Modugno, and M. Inguscio, Fermi-Bose Quantum Degenerate ^{40}K-^{87}Rb Mixture with Attractive Interaction, Phys. Rev. Lett. **89**, 150403 (2002).

[6] Z. Hadzibabic, C. A. Stan, K. Dieckmann, S. Gupta, M. W. Zwierlein, A. Görlitz, and W. Ketterle, Two-Species Mixture of Quantum Degenerate Bose and Fermi Gases, Phys. Rev. Lett. **88**, 160401 (2002).

[7] C.-H. Wu, I. Santiago, J. W. Park, P. Ahmadi, and M. W. Zwierlein, Strongly interacting isotopic Bose-Fermi mixture immersed in a Fermi sea, Phys. Rev. A **84**, 011601(R) (2011).

[8] J. W. Park, C.-H. Wu, I. Santiago, T. G. Tiecke, S. Will, P. Ahmadi, and M. W. Zwierlein, Quantum degenerate Bose-Fermi mixture of chemically different atomic species with widely tunable interactions, Phys. Rev. A **85**, 051602(R) (2012).
[9] I. Ferrier-Barbut, M. Delehaye, S. Laurent, A. T. Grier, M. Pierce, B. S. Rem, F. Chevy, and C. Salomon, A mixture of Bose and Fermi superfluids, Science **345**, 1035 (2014).
[10] X.-C. Yao, H.-Z. Chen, Y.-P. Wu, X.-P. Liu, X.-Q. Wang, X. Jiang, Y. Deng, Y.-A. Chen, and J.-W. Pan, Observation of Coupled Vortex Lattices in a Mass-Imbalance Bose and Fermi Superfluid Mixture, Phys. Rev. Lett. **117**, 145301 (2016).
[11] B. J. DeSalvo, K. Patel, J. Johansen, and C. Chin, Observation of a Degenerate Fermi Gas Trapped by a Bose-Einstein Condensate, Phys. Rev. Lett. **119**, 233401 (2017).
[12] R. Roy, A. Green, R. Bowler, and S. Gupta, Two-Element Mixture of Bose and Fermi Superfluids, Phys. Rev. Lett. **118**, 055301 (2017).
[13] F. Schäfer, N. Mizukami, P. Yu, S. Koibuchi, A. Bouscal, and Y. Takahashi, Experimental realization of ultracold Yb-^{7}Li mixtures in mixed dimensions, Phys. Rev. A **98**, 051602(R) (2018).
[14] M. A. Caracanhas, F. Schreck, and C. M. Smith, Fermi–Bose mixture in mixed dimensions, New J. Phys. **19**, 115011 (2017).
[15] J. Yao, H. Zhai, and R. Zhang, Efimov-enhanced Kondo effect in alkali-metal and alkaline-earth-metal atomic gas mixtures, Phys. Rev. A **99**, 010701(R) (2019).
[16] V. Barbé, A. Ciamei, B. Pasquiou, L. Reichsöllner, F. Schreck, P. S. Żuchowski, and J. M. Hutson, Observation of Feshbach resonances between alkali and closed-shell atoms, Nat. Phys. **14**, 881 (2018).
[17] Y. J. Lin, K. Jiménez-García, and I. B. Spielman, Spin–orbit-coupled Bose–Einstein condensates, Nature (London) **471**, 83 (2011).
[18] P. Wang, Z.-Q. Yu, Z. Fu, J. Miao, L. Huang, S. Chai, H. Zhai, and J. Zhang, Spin-Orbit Coupled Degenerate Fermi Gases, Phys. Rev. Lett. **109**, 095301 (2012).
[19] L. W. Cheuk, A. T. Sommer, Z. Hadzibabic, T. Yefsah, W. S. Bakr, and M. W. Zwierlein, Spin-Injection Spectroscopy of a Spin-Orbit Coupled Fermi Gas, Phys. Rev. Lett. **109**, 095302 (2012).
[20] L. Huang, Z. Meng, P. Wang, P. Peng, S.-L. Zhang, L. Chen, D. Li, Q. Zhou, and J. Zhang, Experimental realization of two-dimensional synthetic spin–orbit coupling in ultracold Fermi gases, Nat. Phys. **12**, 540 (2016).
[21] Z. Wu, L. Zhang, W. Sun, X.-T. Xu, B.-Z. Wang, S.-C. Ji, Y. Deng, S. Chen, X.-J. Liu, and J.-W. Pan, Realization of two-dimensional spin-orbit coupling for Bose-Einstein condensates, Science **354**, 83 (2016).
[22] V. Galitski and I. B. Spielman, Spin–orbit coupling in quantum gases, Nature (London) **494**, 49 (2013).
[23] H. Zhai, Degenerate quantum gases with spin–orbit coupling: A review, Rep. Prog. Phys. **78**, 026001 (2015).
[24] N. R. Cooper, J. Dalibard, and I. B. Spielman, Topological bands for ultracold atoms, Rev. Mod. Phys. **91**, 015005 (2019).
[25] C. Wang, C. Gao, C.-M. Jian, and H. Zhai, Spin-Orbit Coupled Spinor Bose-Einstein Condensates, Phys. Rev. Lett. **105**, 160403 (2010).
[26] J.-R. Li, J. Lee, W. Huang, S. Burchesky, B. Shteynas, F. Ç. Top, A. O. Jamison, and W. Ketterle, A stripe phase with supersolid properties in spin-orbit-coupled Bose-Einstein condensates, Nature (London) **543**, 91 (2017).
[27] W. Zhang and W. Yi, Topological Fulde–Ferrell–Larkin–Ovchinnikov states in spin–orbit-coupled Fermi gases, Nat. Commun. **4**, 2711 (2013).
[28] Z.-Q. Yu and H. Zhai, Spin-Orbit Coupled Fermi Gases across a Feshbach Resonance, Phys. Rev. Lett. **107**, 195305 (2011).
[29] Z.-Y. Shi, X. Cui, and H. Zhai, Universal Trimers Induced by Spin-Orbit Coupling in Ultracold Fermi Gases, Phys. Rev. Lett. **112**, 013201 (2014).
[30] Z.-Y. Shi, H. Zhai, and X. Cui, Efimov physics and universal trimers in spin-orbit-coupled ultracold atomic mixtures, Phys. Rev. A **91**, 023618 (2015).
[31] X. Cui and W. Yi, Universal Borromean Binding in Spin-Orbit-Coupled Ultracold Fermi Gases, Phys. Rev. X **4**, 031026 (2014).
[32] Q. Guan and D. Blume, Three-Boson Spectrum in the Presence of 1D Spin-Orbit Coupling: Efimov's Generalized Radial Scaling Law, Phys. Rev. X **8**, 021057 (2018).
[33] M. Mancini, G. Pagano, G. Cappellini, L. Livi, M. Rider, J. Catani, C. Sias, P. Zoller, M. Inguscio, M. Dalmonte, and L. Fallani, Observation of chiral edge states with neutral fermions in synthetic hall ribbons, Science **349**, 1510 (2015).
[34] B. Song, C. He, S. Zhang, E. Hajiyev, W. Huang, X.-J. Liu, and G.-B. Jo, Spin-orbit-coupled two-electron Fermi gases of ytterbium atoms, Phys. Rev. A **94**, 061604(R) (2016).
[35] E. Braaten and H.-W. Hammer, Universality in few-body systems with large scattering length, Phys. Rep. **428**, 259 (2006).
[36] P. Naidon and S. Endo, Efimov physics: A review, Rep. Prog. Phys. **80**, 056001 (2017).
[37] C. H. Greene, P. Giannakeas, and J. Pérez-Ríos, Universal few-body physics and cluster formation, Rev. Mod. Phys. **89**, 035006 (2017).
[38] V. Efimov, Energy levels of three resonantly interacting particles, Nucl. Phys. A **210**, 157 (1973).
[39] O. I. Kartavtsev and A. V. Malykh, Low-energy three-body dynamics in binary quantum gases, J. Phys. B: **40**, 1429 (2007).
[40] S. Endo, P. Naidon, and M. Ueda, Crossover trimers connecting continuous and discrete scaling regimes, Phys. Rev. A **86**, 062703 (2012).
[41] A. Safavi-Naini, S. T. Rittenhouse, D. Blume, and H. R. Sadeghpour, Nonuniversal bound states of two identical heavy fermions and one light particle, Phys. Rev. A **87**, 032713 (2013).